NeuroImage: Clinical 12 (2016) 277–284

Contents lists available at ScienceDirect

NeuroImage: Clinical

journal homepage: www.elsevier.com/locate/ynicl

Reduced functional connectivity within the primary motor cortex of patients with brachial plexus injury

D. Fraiman[a,b,1], M.F. Miranda[c,1], F. Erthal[j,k], P.F. Buur[d], M. Elschot[d], L. Souza[j,k], S.A.R.B. Rombouts[e,f,g], C.A. Schimmelpenninck[g,h], D.G. Norris[d,i], M.J.A. Malessy[h], A. Galves[c], C.D. Vargas[j,k,*]

[a]Departamento de Matemática y Ciencias, Universidad de San Andrés, Buenos Aires, Argentina
[b]CONICET, Argentina
[c]Instituto de Matemática e Estatística, Universidade de São Paulo, São Paulo, Brazil
[d]Spinoza Centre for Neuroimaging, Amsterdam, The Netherlands
[e]Leiden Institute for Brain and Cognition, Leiden, The Netherlands
[f]Institute of Psychology, Leiden University, Leiden, The Netherlands
[g]Leiden University Medical Center, Department of Radiology, Leiden, The Netherlands
[h]Leiden University Medical Center, Department of Neurosurgery, Leiden, The Netherlands
[i]Erwin L. Hahn Institute for Magnetic Resonance Imaging, University Duisburg-Essen, Essen, Germany
[j]Instituto de Biofísica Carlos Chagas Filho, Universidade Federal do Rio de Janeiro, Brazil
[k]Instituto de Neurologia Deolindo Couto, Universidade Federal do Rio de Janeiro, Rio de Janeiro, Brazil

ARTICLE INFO

Article history:
Received 13 May 2016
Received in revised form 29 June 2016
Accepted 15 July 2016
Available online 26 July 2016

Keywords:
Resting state
Gray matter
Peripheral lesion
Functional connectivity
Horizontal connections
Correlation decay

ABSTRACT

This study aims at the effects of traumatic brachial plexus lesion with root avulsions (BPA) upon the organization of the primary motor cortex (M1). Nine right-handed patients with a right BPA in whom an intercostal to musculocutaneous (ICN-MC) nerve transfer was performed had post-operative resting state fMRI scanning. The analysis of empirical functional correlations between neighboring voxels revealed faster correlation decay as a function of distance in the M1 region corresponding to the arm in BPA patients as compared to the control group. No differences between the two groups were found in the face area. We also investigated whether such larger decay in patients could be attributed to a gray matter diminution in M1. Structural imaging analysis showed no difference in gray matter density between groups. Our findings suggest that the faster decay in neighboring functional correlations without significant gray matter diminution in BPA patients could be related to a reduced activity in intrinsic horizontal connections in M1 responsible for upper limb motor synergies.

1. Introduction

Brain plasticity consists in the ability of the central nervous system (CNS) to modify in response to changes in behavior, as a consequence of skill acquisition or following central/peripheral injury (Buonomano and Merzenich, 1998; Kaas, 1991; Garraghty and Kaas, 1992). Although a growing body of studies shows that plasticity correlates positively with functional recovery following brain injury (review in Cramer et al., 2011), less is known about the mechanisms underlying functional recovery following peripheral lesion and surgical reconstruction.

Severe traumatic brachial plexus lesions with root avulsion (BPA) leads to motor and sensory function loss of the arm. Although the reconstruction of the original peripheral nerve pathways is not possible, nerve transfer can be performed to regain function. For instance, by connecting the distal denervated musculocutaneous (MC) nerve to the third to sixth thoracic intercostal (IC) nerves (Midha, 2004). Normally the IC nerves are connected to intercostal muscles, which are involved in volitional breathing and postural control. After successful reinnervation of the biceps muscle following intercostal-musculocutaneous (ICN-MC) nerve transfer, the ICN now innervates the biceps muscle. Initially, elbow flexion by biceps contraction can only be effected by respiratory effort, for instance sustained inspiration. In time however, volitional control becomes possible, implying a change in control. Following this surgical procedure, about two-thirds of patients regain biceps function with at least Grade 3 out of 5 according to the Medical Research Council scale (Seddon; Narakas and Hentz, 1988; Malessy et al., 1993; Malessy and Thomeer, 1998; Midha, 2004).

Applying transcranial magnetic stimulation (TMS) to the primary motor cortex (M1), Mano et al. (1995) and Malessy and Thomeer (1998) studied the change in control over the reinnervated biceps muscle some years after ICN-MC transfer performed in patients with BPA. M1 contains a map of movements organized somatotopically (Rasmussen and Penfield, 1950) with gross and largely separated

* Corresponding author at: Instituto de Biofísica Carlos Chagas Filho, Universidade Federal do Rio de Janeiro, Rio de Janeiro, Brazil.
E-mail address: cdvargas@biof.ufrj.br (C.D. Vargas).
[1] The authors equally contributed to this article.

http://dx.doi.org/10.1016/j.nicl.2016.07.008

body part subdivisions represented sequentially from lateral to medial precentral gyrus. Mano et al. (1995) and Malessy and Thomeer (1998) found in these operated patients that the biceps representation shifted from medial to a more lateral position (i.e a shift from the trunk area to the arm area) in M1. Although plausible hypotheses have been put forward to understand the role of brain plasticity in recovery of BPA patients after ICN-MC nerve transfer (Mano et al., 1995; Malessy and Thomeer, 1998; Malessy et al., 2003), it remains unclear which mechanisms underlie the shift from respiratory dependent biceps control to volitional biceps control and to what extent this functional change is a result of plastic changes in the brain.

Horizontal intrinsic connections between spatially distant and functionally different parts of M1 have been consistently revealed in animal models (Huntley and Jones, 1991; Jacobs and Donoghue, 1991; Sanes and Donoghue, 2000; Ziemann, 2004). These long-range horizontal connections were proposed to be involved in activity synchronization beyond cortical modules (Boucsein et al., 2011), fine motor synergy coordination (review in Schieber, 2001) and use-dependent motor learning (review in Sanes and Donoghue, 2000). Such horizontal network within M1 might also underlie plastic modifications induced by BPA and nerve transfer.

Resting-state fMRI has already been used to investigate how the human brain's functional organization is affected by BPA (Liu et al., 2013; Qiu et al., 2014). Herein we aim at the effects of BPA on local functional connectivity by exploring the decay of the functional correlations between neighboring voxels within M1. We find evidence that these correlations decay faster as a function of distance in BPA patients as compared to the control group in the M1 region corresponding to the arm but not to the face area. We also investigate whether such larger correlation decay in patients can be attributed to a gray matter diminution in M1 by means of structural imaging analysis. The lack of difference in gray matter density between BPA group and control together with the faster correlation decay in neighboring functional correlations in BPA patients suggests a reduced activity in intrinsic functional connections responsible for upper limb motor synergies in M1.

2. Material and methods

2.1. Subjects

Nine right-handed patients with a brachial plexus lesion (mean age 34.6, SD = 4.8; mean age at lesion: 18.8 ± 2.2) and eleven right-handed control subjects (mean age 35.4 ± 8 years), matched in age and sex with the patient's group participated in the study. All patients suffered a brachial plexus traction lesion with root avulsion on the right side. They were included in the study only if they had undergone successful Intercostal to Musculocutaneous (ICN-MC) nerve transfer, meaning there was at least some recovery of biceps function (grade of 1 or higher as measured with the Medical Research Council grade). At the time of the study they showed variable degrees of biceps function recovery (Mean: 3.0, SD 1–4, as measured with the Medical Research Council grade). The exclusion criteria were history of neurological trauma and additional surgical procedures aimed at regaining elbow flexion (e.g. Steindler flexorplasty), and general exclusion criteria for MRI scanning (such as claustrophobia, pacemaker, and metallic implants). The local ethics committee approved the study and the patients gave written informed consent in accordance with the declaration of Helsinki. Information about patients and controls are presented in Tables 1 and 2.

2.2. Experimental procedure

The volunteers were comfortably positioned inside the scanner during the experiment. Pillows were placed between the forehead of the subject and the coil to minimize head movement. Lower arms were positioned next to the body at a comfortable angle between 10° and 30° by using cushions. The palm of subjects' hands faced up to the extent that this was possible without causing discomfort. Subjects were instructed to keep their eyes closed, and not to think of anything in particular during resting-state scanning. The scanning time lasted for 5 min.

Table 1
Information of the patients with braquial plexus lesion. Injury type classification includes Avulsion (Av.) and Neurotmesis (Nt.) types. I1 is the time interval in months between lesion and surgery. I2 is the time interval in years between surgery and fMRI scan.

Id	Age at scan	Gender	Injury type	Age at lesion	I1	I2	Location
P01	35	M	Av. C5-T1	16	2	19	Leiden
P02	40	M	Av. C5-C7	35	11.2	5	Leiden
P03	36	M	Av. C5-T1	18	4	18	Leiden
P04	38	F	Av. C5-C7	22	2.8	16	FCDC
P05	33	F	Av. C5-C7	19	2	14	Leiden
P06	32	M	Av. C5-C7	26	5.1	6	FCDC
P07	40	M	Av. C6-C7 Nt. C5	23	3	17	Leiden
P08	40	M	Av. C6-T1 Nt. C5	26	1	14	FCDC
P09	26	M	Av. C5-T1	19	5	7	FCDC

2.3. Data acquisition

To reduce travel time and thereby maximize the willingness of the patients to participate in the study, data from control participants and from patients were acquired at two centers in the Netherlands. Six control and four patients underwent scanning at Donders Institute (DI) in Nijmegen and five controls and five patients, at the Leiden University Medical Center (LUMC). At the Donders Institute (DI) in Nijmegen, measurements were performed on a 3 T TIM Trio MR scanner (Siemens Medical Solutions, Erlangen, Germany). At the Leiden University Medical Center (LUMC), a 3 T Achieva scanner (Philips Medical Systems, Best, The Netherlands) was used. On both systems an eight-channel head coil, which was produced by the same vendor, was used for all data collection. Acquisition parameters were adjusted to be as equal as possible between the two scanners, while still having near optimal settings for each system.

Resting-state fMRI data were acquired with a 2D single-shot EPI sequence. The whole brain was covered by acquiring 38 axial slices (3.5 mm isotropic voxels, 0.35 mm interslice gap, 64 × 64 matrix). Flip angle = 85°, volume repetition time = 2180 ms, echo time = 30 ms. An in-plane parallel imaging acceleration factor of 2 was used. Online image reconstruction was performed using the GRAPPA [REF 37] and SENSE algorithms [REF 38] on the Siemens and Philips systems, respectively. A number of 220 volumes were acquired for a total acquisition time of 8 min.

2.4. Data analysis

2.4.1. Resting state fMRI data pre-processing

The statistical parametric mapping software package (SPM8, Wellcome Department of Cognitive Neurology, London) was used for

Table 2
Information of the control group. Control group and patients group match in age (p-value for unpaired t-test is 0.7996) and proportion of each gender (p-value for proportion z-test is 0.4132).

Id	Age	Gender	Location
C01	50	M	FCDC
C02	31	M	FCDC
C03	34	M	FCDC
C04	31	M	Leiden
C05	31	M	Leiden
C06	39	M	FCDC
C07	40	M	FCDC
C08	28	M	FCDC
C09	33	F	Leiden
C10	31	M	Leiden
C11	36	M	Leiden

part of the pre-processing of resting state fMRI data. The first three functional volumes of each run were removed to eliminate non-equilibrium magnetization effects. The remaining images were corrected for head movement by realigning them to the mean image via rigid body transformations. They were subsequently band-pass filtered (0.01–0.05 Hz) to remove physiological noise. Functional images were co-registered to anatomical images for every subject. Finally, brain images were normalized to standard MNI 152 template using FLIRT (from FSL software, (Smith et al., 2009)) and data was resampled to 2 mm × 2 mm × 2 mm resolution. Masks from both the right and the left primary motor cortices (M1) were taken from Geyer et al. (1996). These masks had MNI coordinates equivalent to those of the functional brain images employed herein. To compare control subjects and patients within the body map representation the mask was segmented in five sub-regions delimited by four saggital planes (Fig. 1A). These saggital planes are located in each color change in Fig. 1A. Since our main interest was to investigate the functional relationship between neighboring voxels, these sub-regions were constructed so that the number of voxels should be roughly the same (Fig. 1B). Due to the natural irregularity in M1 cortical thickness, this choice led to a different number of slices in the sagittal dimension (Fig. 1C) as well as some variability in the maximum distance between voxels (Fig. 1D).

We designed an analysis to investigate local interactions between voxels within the sub-masks of M1. Our goal was is to understand how interactions decay as a function of the distance between voxels, and most importantly, to compare the correlation behavior between BPA's and controls. The degree of functional interaction between two voxels was calculated using the Spearman (rank) correlation. This is a non-linear measure of correlation, and it is equal to the Pearson correlation between the rank values of the two variables studied. It assesses how well the relationship between two variables can be described using a monotonic function, while Pearson correlation assesses linear relationships. Moreover, the Spearman correlation has the advantage to be hardly affected by an outlier whereas the Pearson correlation will be greatly affected. For each sub-region of M1 we proceeded as follows. For every voxel on the sub-region, we computed its correlation with all other voxels. Precisely, let $X_t(v)$ represent the value of the resting state BOLD response in voxel v at time t, for $t \in \{1,2,\ldots,T\}$, and let $R_t(v)$ be the rank of $X_t(v)$. Given two voxels v and v', the Spearman correlation between $(X_1(v),\ldots,X_T(v))$ and $(X_1(v'),\ldots,X_T(v'))$ is defined as the Pearson correlation between the ranked time series $(R_1(v),\ldots,R_T(v))$ and $(R_1(v'),\ldots,R_T(v'))$. After all the computations were performed, we had for each voxel two associated quantities: 1) the estimated Spearman correlation coefficient computed between that voxel and remaining ones (one quantity for each pair), and 2) the Euclidean distance between each pair of voxels (Garcia-Cordero et al., 2015). In the next paragraph we describe in detail how the computations were performed.

Following the aforementioned computations, we calculated for each obtained distance: 1) the average of the correlation coefficient, and 2) the corresponding 95% confidence interval. These calculations were performed for each sub-regions and for both groups, controls and BPA's (Fig. 2A–E). Further, for each distance, we compared the correlations between the two groups (control versus BPA's), using a Wilcoxon rank-sum test. The goal was to identify if these correlations have a different behavior in the two groups (Fig. 2F).

Since we were performing one hypothesis tests for each point in distance (total of 70 points of distance that range from 1 to 10 in voxels), we applied a multiple comparisons correction. The corrected threshold was obtained based on the Benjamini-Hochberg procedure (Benjamini and Hochberg, 1995), that controls the false discovery rate $\alpha = 0.05$ for the 70 tests performed in each submask. Let us call $H(m)$ the m-th

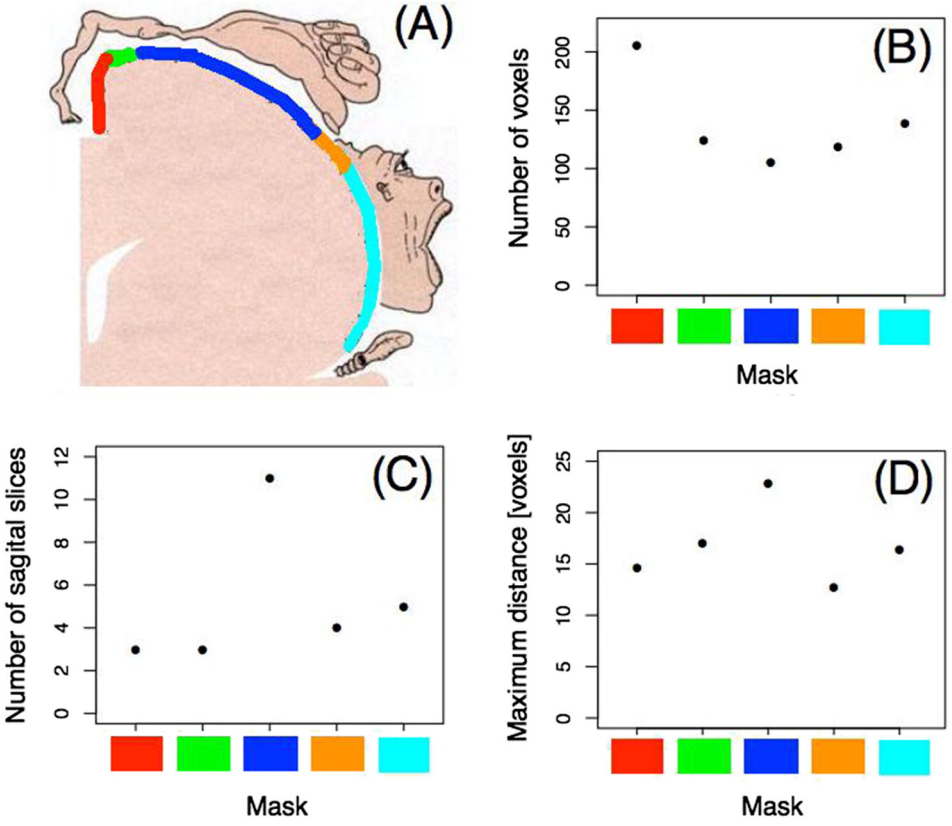

Fig. 1. Masks in the primary motor cortex (M1). A) Pictorial representation of the human body map in the right M1 (obtained from http://www.grandesimagenes.com/homunculo/). Each color indicates a mask within M1. B) Number of voxels per mask is roughly equivalent; C) Number of slices in the sagittal plane within the masks; D) Maximum distance between the voxels per mask. (For interpretation of the references to color in this figure, the reader is referred to the web version of this article.)

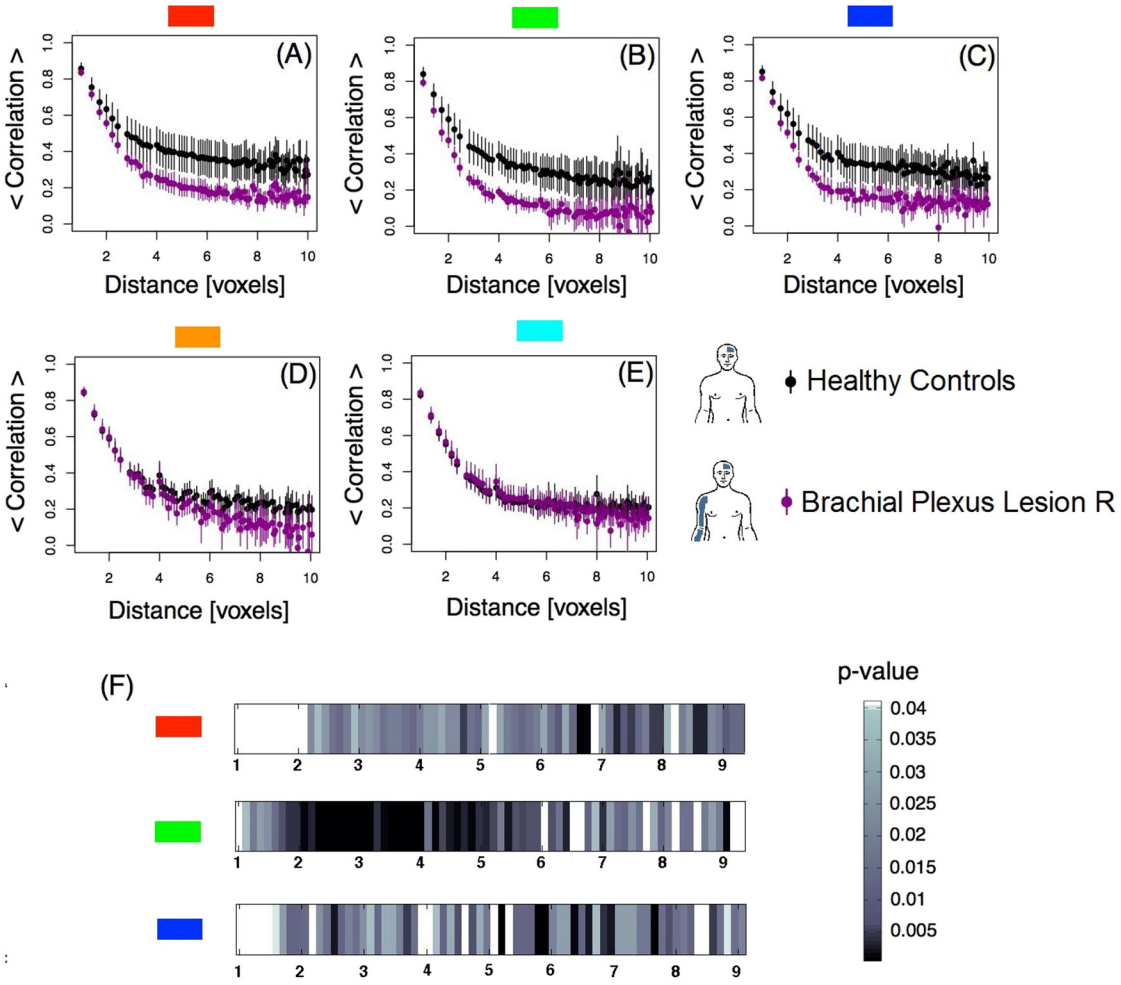

Fig. 2. Left hemisphere, contralateral to BPA — Pairwise Spearman's rank correlation coefficient between voxels as a function of distance in voxels. A-E: Average correlations per mask as a function of distance between voxels plotted for control subjects and BPA patients. The bars represent the 95% confidence interval. F) Chart representing the level of statistical significance (p-value) resulting from the comparison of the average correlations between groups within masks A, B, and C as a function of distance. Masks D and E did not show any significant difference between the two groups. (For interpretation of the references to color in this figure, the reader is referred to the web version of this article.)

null hypotheses, for $m = 1, \ldots, 70$. The procedure consisted on the following steps: 1) we ordered the p-values and let $p(k)$ denote the k-th ordered p-value; 2) for $\alpha = 0.05$, we found the largest k such that $p(k) \leq k\alpha/m$, where m is the number of multiple tests (in our case m = 70); 3) we rejected all $H(j)$ for $j = 1, \ldots, k$.

2.5. Structural MRI

The original T1-weighted images of size 198 × 256 × 256 mm3 (voxel size: $1 \times 1 \times 1$ mm^3) were analyzed. These anatomical images were obtained using the MP RAGE sequence at the FCDC (TR/TE = 2300 / 3.03 ms, 192 sagittal slices, 1.0 × 1.0 × 1.0 mm voxels, FOV = 256 mm, 256 × 256 matrix, acceleration factor = 2, GRAPPA reconstruction) and at the LUMC (TR/TE = 1935 / 5.59 ms, 140 transverse slices, 0.875 × 0.875 × 1.2 mm voxels, FOV = 224 mm, 256 × 256 matrix). The images were pre-processed using FSL (FMRIB Software Library) and the steps included brain extraction (using BET), linear registration into the MNI152 space (using FLIRT library), and finally the images were segmented into white matter, gray matter and cerebrospinal fluid (using FAST with main MRF parameter equal to zero). The same M1 mask employed to extract pairwise correlations described above (Geyer et al., 1996) was employed to test whether the gray matter tissue on the motor cortex differs among subjects with brachial plexus injury and the control group. After the pre-processing steps, each voxel on the gray matter tissue map contained a value in the range 0–1 that represents the proportion of that tissue present in that voxel. To identify morphological differences in M1 associated with brachial plexus injury, a Bayesian Spatial Transformation Model (STM) (Miranda et al., 2013) was fitted with the gray matter as the response variable and a covariate vector containing the intercept and diagnostic status (1 for brachial plexus injury and −1 for control). Common voxel-wise methods such as VBM treat voxels as independent units, ignoring important spatial smoothness during the estimation procedure. The STM method used to analyze the structural images is a Bayesian hierarchical model that simultaneously accounts for the varying amount of smoothness across the imaging space and the normality assumption in the model. For each voxel v in M1, the model estimates the posterior probability distribution of $\beta(v)$, the coefficient associated with diagnostic status (Miranda et al., 2013). Based on the posterior probability, we compute a 95% interval for $\beta(v)$ by considering the quantiles of its posterior distribution. This interval is known as a credible interval and its interpretation is different than that of a confidence interval. As an example, suppose that the 95% credible interval for $\beta(v)$ is $[a,b]$. We can say that the probability of the coefficient $\beta(v)$ be in the interval $[a,b]$ is 0.95. We can further use these intervals to make a decision. If the interval contains 0 and since $\beta(v)$ represents the difference between controls and BPAs for a particular voxels v, we conclude that there is no difference in the gray mater tissue proportion when we compare patients with brachial plexus injury and controls. We repeat the same procedure for all voxels v in M1.

3. Results

For each sub-region within M1, we were interested in investigating whether correlation behavior was different for BPA patients and controls. Our assumption was that for BPA patients the long-range correlations, i.e. correlation between far away voxels, would lose strength.

To investigate this assumption, we computed the Pairwise Spearman's rank correlation between voxels as described in the previous section. We then plotted the correlation as a function of distance (in voxels units) for each M1 submask contralateral to the affected limb (left hemisphere) for controls and BPA patients. Results are shown in Fig. 2. Panels A–E exhibit that the correlation function decays from high values for closer voxels to low levels at relatively large distance. This happened in all five regions and for both groups. A closer inspection shows a difference among groups (non-overlapping confidence intervals) for the red (panel A), green (panel B) and dark blue (panel C) masks. These medial regions correspond roughly to the trunk, upper body and hand, as depicted in the homunculus (Fig. 1). These differences are statistically significant as confirmed by the Wilcoxon rank-sum test performed (see Section 2.4). The statistical results are shown in Fig. 2F and Fig. A.5 in Appendix A. After correction for multiple comparisons, the threshold values for masks A, B and C is 0.04. The highest differences among controls and BPA patients are observed at the green mask at distances of approximately 6 to 10 mm (3 to 5 voxels). No difference between groups is evident in the D and E masks (orange and light blue areas), which corresponds roughly to the neck/face representation in M1.

We also compared the subsamples of patients with low ($n = 4$, MRC grade 0, 1,2) and high ($n = 5$, MRC 4, see Table 1) degree of functional recovery after surgical reconstruction. We took the same steps described above when we compared controls and BPI's. In each of the 5 masks, data did not show any difference in the correlation behavior between patients with low and high degree of functional recovery.

Since changes of interhemispheric functional connectivity between motor areas were recently reported in patients with BPA (Liu et al., 2013), we also investigated whether these effects were present in our cohort. We performed a similar analysis for each sub-region in M1 in the hemisphere ipsilateral to the affected limb for controls and BPA patients. Results are shown in Fig. 3. Fig. 3A–E shows differences between controls and BPA patients (non-overlapping confidence intervals) for the red (Fig. 3A) and dark blue (Fig. 3C) masks. These differences were confirmed by performing a Wilcoxon rank-sum test. Results for the Wilcoxon test are shown in Fig. 3F and Fig. A.6 in Appendix A. After correction for multiple comparisons, the threshold values for the red mask (Fig. 3A) is 0.04 and the dark blue mask (3C) is 0.02.

Finally, we investigated if the observed differences in the correlation functions were accompanied by differences in gray matter density. To verify if there was any structural difference in M1 between groups, structural imaging analysis was performed using STM (see Material and methods). Results are shown in Fig. 4. Inspecting the figure, we notice that for all voxels included in the model, the posterior mean is close to zero, indicating a lack of difference between controls and BPA patients. We further computed the 95% credible interval for each voxel and all of them, with no exception, included the value zero. Such result

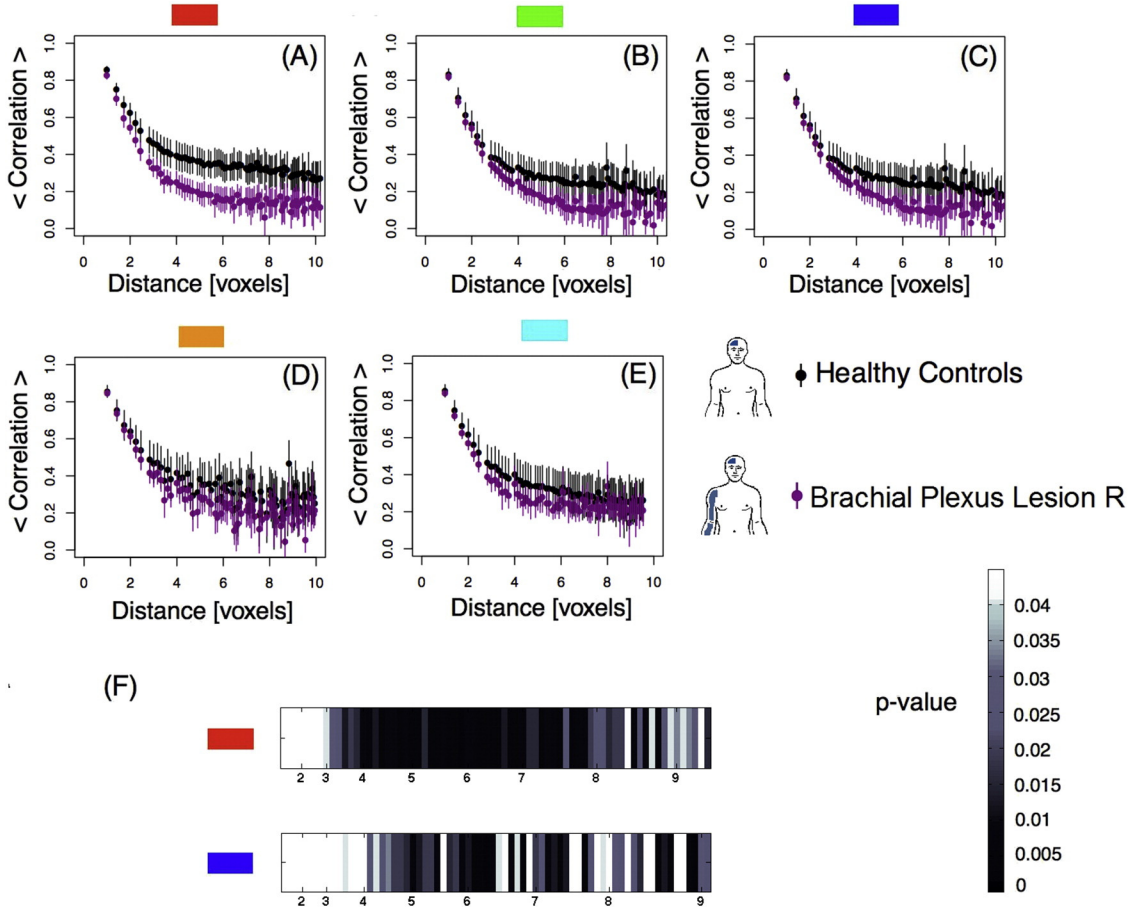

Fig. 3. Right hemisphere, ipsilateral to BPA — Pairwise Spearman's rank correlation coefficients between voxels as a function of distance in voxels. A–E: Average correlations per mask as a function of distance between voxels plotted for control subjects and BPA patients. The bars represent the 95% confidence interval. F) Chart representing the level of statistical significance (p-value) resulting from the comparison of the average correlations between groups within masks A and C as a function of distance. Masks B, D and E did not show any significant difference between the two groups. (For interpretation of the references to color in this figure, the reader is referred to the web version of this article.)

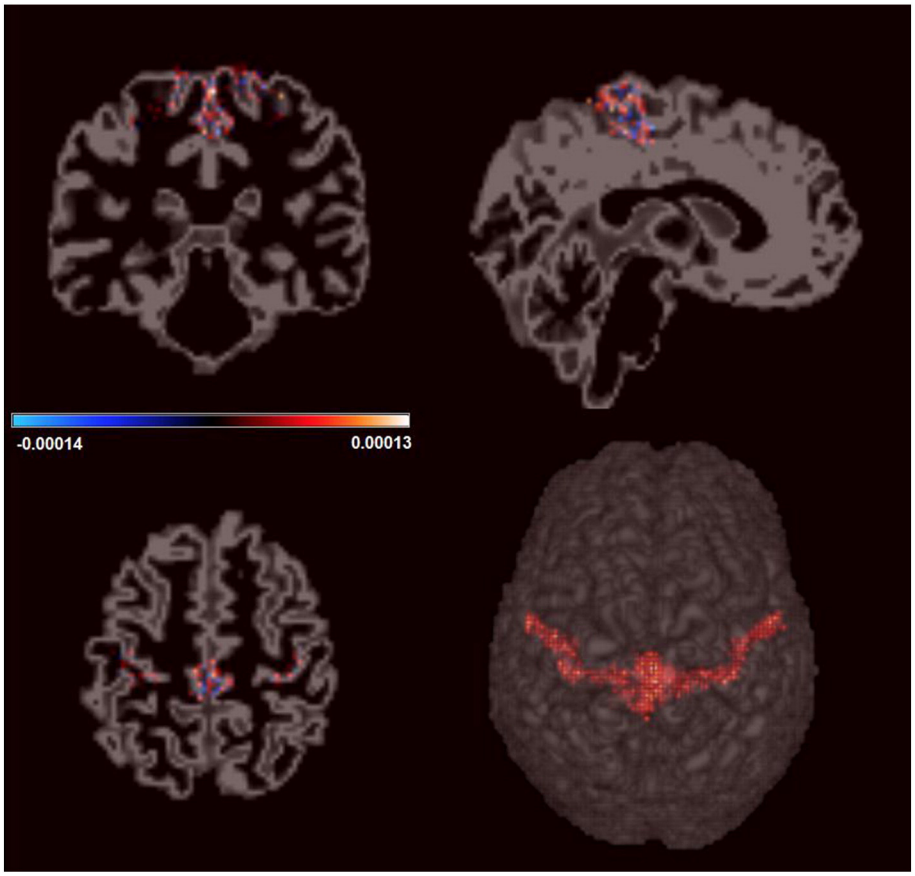

Fig. 4. Estimates for the differences in M1 gray matter tissue density between BPA and control group. For each voxel, the color represents the posterior mean estimate of the coefficients associated with the Control versus BPA contrast. As observed in the color bar the values are close to zero indicating that the gray matter density does not differ between groups.

confirms that there are no significant differences in gray matter tissue between BPA patients and the control group.

4. Discussion

We herein investigated the correlation decay between neighboring voxels during resting state in the primary motor cortex (M1). We compared control volunteers to patients that had a traumatic brachial plexus lesion with root avulsions (BPA) in adulthood in whom an intercostal to musculocutaneous (ICN-MC) nerve transfer was performed.

Analyzing correlation as a function of distance between points in space is a classical tool in spatial statistics (Gelfand et al., 2010; Sherman, 2011) and in statistical physics. A typical approach to describe an interacting system is to study how the interactions (measured, for example, by linear correlation) decay with increasing distance. In general, mutual dependence between two units of a system (in our case, voxels) decreases the further apart they are. This methodology has been recently employed to compare control subjects and stroke patients (Garcia-Cordero et al., 2015). Applied to the present results, changes in the interactions between voxels in M1 should correspond to functional reorganization due to BPA. Accordingly, the analysis of the correlation function between voxels revealed a faster decay in the M1 region corresponding to the trunk/arm in BPA patients as compared to the control group.

Functional connectivity differences were found between healthy controls and BPA injured patients in M1. These differences were most evident in the masks corresponding roughly to the upper limb and trunk representations. However no difference between groups was detected in the mask region corresponding to the face representation, indicating that these changes were specific to body segment representations more directly affected by BPA. A fine grain statistical comparison between groups showed highest differences in pairwise correlations among controls and BPA patients at distances of approximately 6 to 10 mm (3 to 5 voxels).

Whereas the higher functional correlation found in M1 for spatially close voxels could result from intense functional interaction occurring within local modules, lower correlation values observed between voxels at higher distance might result from comparatively lower levels of concerted activity within M1. Spanning several millimeters within M1, long-range horizontal connections were proposed to be involved in activity synchronization beyond cortical modules (Boucsein et al., 2011), fine motor synergy coordination (review in Schieber, 2001) and use-dependent motor learning (review in Sanes and Donoghue, 2000). Consequently, the reduced pairwise correlation values found mostly for larger distances in M1 after BPA are possibly due to decreased activity in horizontal connections, as a result of greatly reduced upper arm and trunk motor synergies. Thus, by strongly disrupting upper limb motor synergies (Schieber, 2001), denervation due to BPA would affect long-range connections and strongly reduce functional connectivity within M1. Accordingly, we recently showed that brachial plexus injured patients show altered postural control (Souza et al., 2015).

Reduced pairwise correlations were also verified at regions corresponding to the trunk and hand areas in M1 ipsilateral to the affected limb, indicating interhemispheric effects of BPA. These results are in accordance with a resting state functional connectivity approach recently used to explore changes of interhemispheric functional connectivity of motor areas in patients with BPA (Liu et al., 2013). Indeed, in healthy subjects, enhancing the proprioceptive input of a hand muscle by applying a low amplitude vibration was shown to reduce corticospinal excitability of the contralateral homologous muscle, suggesting transcallosal effects (Swayne et al., 2006). Likewise, interhemispheric inhibition has recently been verified for forearm muscles in healthy subjects (Ibey et

al., 2015). Finally, changes in the cortical representation of the intact limb have also been proven in lower limb amputees (Simoes et al., 2012). Thus, in BPA patients changes in transcallosal connectivity might have resulted in reduced pairwise correlation also in the trunk/hand representations of M1 ipsilateral to the affected limb.

Pairwise correlation decay as a function of distance was found to occur similarly in patients with low (MRC grade 1 and 2) and high degree (MRC 4) of functional recovery after surgical reconstruction. These results, although obtained with small subsamples, could suggest that long-range horizontal connections do not play a prominent role in functional control following reinnervation. In any case, the severe diminution of the correlation between voxels at intermediate distances observed within M1 could be attributed to the massive missing of sensorimotor connections with the parts of the arm that have not been surgically reconnected. This in turn would occur in parallel to a greatly reduced repertoire of upper limb synergies (review in Dy et al., 2015).

Mano et al. were the first to investigate the location of the cortical area responsible for contraction of the reinnervated biceps muscle in BPA patients using TMS (Mano et al., 1995). Stimulating the motor area situated medially to the cortical area evoking a response in the healthy biceps resulted in a motor evoked potential (MEP) in the reinnervated biceps. At the end stage of recovery, however, the cortical area evoking responses in the biceps had shifted laterally in the motor cortex towards the deefferented biceps area (Mano et al., 1995). Malessy and Thomeer (1998) also did not find any difference between the TMS evoked 'cortical location' of the reinnervated and normal biceps areas. Employing fMRI, Malessy et al. (2003) confirmed that the cortical regions in M1 activated during contraction of the surgically reinnervated and the healthy biceps were topologically equivalent. Thus, during recovery, a medial-to-lateral cortical shift might represent a shift from the trunk area to the arm area, possibly underlying the decoupling of volitional breathing from biceps control. One could conjecture that such cortical shift might be endowed by the recruitment of horizontal connections within M1. These effects might however be subtle enough to fall below our detection threshold. Thus, how these plastic changes relate to reduced correlation function found herein deserves further investigation.

Importantly, the differences found between controls and BPA injured patients in M1 were not accompanied by gray matter changes. Accordingly, so far peripheral lesions were shown to drive anatomical changes (as measured by gray matter modifications in MRI) in several brain regions such as primary somatosensory cortex, secondary somatosensory cortex, ventrolateral prefrontal cortex, middle cingulate cortex, anterior cingulate cortex and thalamus (Taylor et al., 2009; Davis et al., 2011; Jaggi and Singh, 2011) but not in M1. The reasons for such departure are unknown. In conclusion, the faster decay in functional correlations without any gray matter diminution in BPA patients clearly indicates a reduced activity in intrinsic M1 connectivity. This could result from a BPA-induced dysfunction in the horizontal connection intrinsic network, considered to be responsible both of coordinating upper limb motor synergies and driving plastic changes in M1.

Supplementary data to this article can be found online at http://dx.doi.org/10.1016/j.nicl.2016.07.008.

Acknowledgements

This work is part of University of São Paulo (USP) project Mathematics, computation, language and the brain, Fundação de amparo a pesquisa do Estado de São Paulo (FAPESP) project NeuroMat (grant 2013/07699-0), CAPES NUFFIC (038/12), Conselho Nacional de Pesquisa (CNPq) (grants 480108/2012-9 and 478537/2012-3), Fundação de amparo a pesquisa do Rio de Janeiro FAPERJ (grants E-26/111.655/2012 and E-26/110.526/2012) and Programa de apoyo a la investigacion de la Universidad San Andre's (PAI UdeSA). The funders had no role in study design, data collection and analysis, decision to publish, or preparation of the manuscript.

References

Benjamini, Y., Hochberg, Y., 1995. Controlling the false discovery rate: a practical and powerful approach to multiple testing. J. R. Stat. Soc. Ser. B Methodol. 57 (1), 289–300. http://dx.doi.org/10.2307/2346101.

Boucsein, C., Nawrot, M.P., Schnepel, P., Aertsen, A., 2011. Beyond the cortical column: abundance and physiology of horizontal connections imply a strong role for inputs from the surround. Front. Neurosci. 5, 32.

Buonomano, D.V., Merzenich, M.M., 1998. Cortical plasticity: from synapses to maps. Annu. Rev. Neurosci. 21, 149–186.

Cramer, S.C., Sur, M., Dobkin, B.H., O'Brien, C., Sanger, T.D., Trojanowski, J.Q., Rumsey, J.M., Hicks, R., Cameron, J., Chen, D., Chen, W.G., Cohen, L.G., deCharms, C., Duffy, C.J., Eden, G.F., Fetz, E.E., Filart, R., Freund, M., Grant, S.J., Haber, S., Kalivas, P.W., Kolb, B., Kramer, A.F., Lynch, M., Mayberg, H.S., McQuillen, P.S., Nitkin, R., Pascual-Leone, A., Reuter-Lorenz, P., Schiff, N., Sharma, A., Shekim, L., Stryker, M., Sullivan, E.V., Vinogradov, S., 2011. Harnessing neuroplasticity for clinical applications. Brain 134 (Pt 6), 1591–1609.

Davis, K.D., Taylor, K.S., Anastakis, D.J., 2011. Nerve injury triggers changes in the brain. Neuroscientist 17 (4), 407–422.

Dy, C., Garg, R., Lee, S., Tow, P., Mancuso, C., Wolfe, S., 2015. A systematic review of outcomes reporting for brachial plexus reconstruction. J. Hard Surg. Am. 40 (2), 308–313. http://dx.doi.org/10.1016/j.jhsa.2014.10.033.

Garcia-Cordero, I., Sedeno, L., Fraiman, D., Craiem, D., de la Fuente, L.A., Salamone, P., Serrano, C., Sposato, L., Manes, F., Ibanez, A., 2015. Stroke and neurodegeneration induce different connectivity aberrations in the insula. Stroke 46 (9), 2673–2677.

Garraghty, P.E., Kaas, J.H., 1992. Dynamic features of sensory and motor maps. Curr. Opin. Neurobiol. 2 (4), 522–527.

Gelfand, A., Fuentes, M., Guttorp, P., Diggle, P., 2010. Handbook of Spatial Statistics, Chapman & Hall/CRC Handbooks of Modern Statistical Methods. Taylor & Francis URL http://books.google.com/books?id=EFbbcMFZ2mMC.

Geyer, S., Ledberg, A., Schleicher, A., Kinomura, S., Schormann, T., Burgel, U., Klingberg, T., Larsson, J., Zilles, K., Roland, P.E., 1996. Two different areas within the primary motor cortex of man. Nature 382 (6594), 805–807.

Huntley, G.W., Jones, E.G., 1991. Relationship of intrinsic connections to forelimb movement representations in monkey motor cortex: a correlative anatomic and physiological study. J. Neurophysiol. 66 (2), 390–413.

Ibey, R.J., Bolton, D.A., Buick, A.R., Staines, W.R., Carson, R.G., 2015. Interhemispheric inhibition of corticospinal projections to forearm muscles. Clin. Neurophysiol. 126 (10), 1934–1940.

Jacobs, K.M., Donoghue, J.P., 1991. Reshaping the cortical motor map by unmasking latent intracortical connections. Science 251 (4996), 944–947.

Jaggi, A.S., Singh, N., 2011. Role of different brain areas in peripheral nerve injury-induced neuropathic pain. Brain Res. 1381, 187–201.

Kaas, J.H., 1991. Plasticity of sensory and motor maps in adult mammals. Annu. Rev. Neurosci. 14, 137–167.

Liu, B., Li, T., Tang, W.J., Zhang, J.H., Sun, H.P., Xu, W.D., Liu, H.Q., Feng, X.Y., 2013. Changes of inter-hemispheric functional connectivity between motor cortices after brachial plexuses injury: a resting-state fMRI study. Neuroscience 243, 33–39.

Malessy, M.J., Thomeer, R.T., 1998. Evaluation of intercostal to musculocutaneous nerve transfer in reconstructive brachial plexus surgery. J. Neurosurg. 88 (2), 266–271.

Malessy, M.J., Bakker, D., Dekker, A.J., Van Duk, J.G., Thomeer, R.T., 2003. Functional magnetic resonance imaging and control over the biceps muscle after intercostal-musculocutaneous nerve transfer. J. Neurosurg. 98 (2), 261–268.

Malessy, M.J., van Dijk, J.G., Thomeer, R.T., 1993. Respiration-related activity in the biceps brachii muscle after intercostal-musculocutaneous nerve transfer. Clin. Neurol. Neurosurg. 95 (Suppl.), 95–102.

Mano, Y., Nakamuro, T., Tamura, R., Takayanagi, T., Kawanishi, K., Tamai, S., Mayer, R.F., 1995. Central motor reorganization after anastomosis of the musculocutaneous and intercostal nerves following cervical root avulsion. Ann. Neurol. 38 (1), 15–20.

Midha, R., 2004. Nerve transfers for severe brachial plexus injuries: a review. Neurosurg. Focus. 16 (5), E5.

Miranda, M.F., Zhu, H., Ibrahim, J.G., 2013. Bayesian spatial transformation models with applications in neuroimaging data. Biometrics 69 (4), 1074–1083.

Narakas, A.O., Hentz, V.R., 1988. Neurotization in brachial plexus injuries. Indication and results. Clin. Orthop. Relat. Res. 1 (237), 43–56.

Qiu, T.M., Chen, L., Mao, Y., Wu, J.S., Tang, W.J., Hu, S.N., Zhou, L.F., Gu, Y.D., 2014. Sensorimotor cortical changes assessed with resting-state fMRI following total brachial plexus root avulsion. J. Neurol. Neurosurg. Psychiatry 85 (1), 99–105.

Rasmussen, T., Penfield, W., 1950. The Cerebral Cortex of Man. A Clinical Study of Localization of Function. Macmillan, New York.

Sanes, J.N., Donoghue, J.P., 2000. Plasticity and primary motor cortex. Annu. Rev. Neurosci. 23, 393–415.

Schieber, M.H., 2001. Constraints on somatotopic organization in the primary motor cortex. J. Neurophysiol. 86 (5), 2125–2143.

Seddon, H.J., 2005. Peripheral Nerve Injuries, Medical Research Council Special Report Series. 282.

Sherman, M., 2011. Statistics and Spatio-temporal Data: Covariance Functions and Directional Properties. Wiley, Chichester, West Sussex, U.K. URL http://isbnplus.org/9780470699584.

Simoes, E.L., Bramati, I., Rodrigues, E., Franzoi, A., Moll, J., Lent, R., Tovar-Moll, F., 2012. Functional expansion of sensorimotor representation and structural reorganization of callosal connections in lower limb amputees. J. Neurosci. 32 (9), 3211–3220.

Smith, S.M., Fox, P.T., Miller, K.L., Glahn, D.C., Fox, P.M., Mackay, C.E., Filippini, N., Watkins, K.E., Toro, R., Laird, A.R., Beckmann, C.F., 2009. Correspondence of the brain's functional architecture during activation and rest. Proc. Natl. Acad. Sci. U. S. A. 106 (31), 13040–13045.

Souza, L., Lemos, T., Silva, D.C., de Oliveira, J.M., Guedes Correa, J.F., Tavares, P.L., Oliveira, L.A., Rodrigues, E.C., Vargas, C.D., 2015. Balance impairments after brachial plexus injury as assessed through clinical and posturographic evaluation. Front. Hum. Neurosci. 9, 715.

Swayne, O., Rothwell, J., Rosenkranz, K., 2006. Transcallosal sensorimotor integration: effects of sensory input on cortical projections to the contralateral hand. Clin. Neurophysiol. 117 (4), 855–863.

Taylor, K.S., Anastakis, D.J., Davis, K.D., 2009. Cutting your nerve changes your brain. Brain 132 (Pt 11), 3122–3133.

Ziemann, U., 2004. TMS induced plasticity in human cortex. Rev. Neurosci. 15 (4), 253–266.